MRS Communications

https://doi.org/10.1557/s43579-022-00238-w

MRS Communications

Computational Approaches for Materials Discovery and Development Research Letter

A finite-temperature coarse-grained atomistic approach for understanding the kink-controlled dynamics of micrometer-long dislocations in high-Peierls-barrier materials

Rigelesaiyin Ji, and Thanh Phan, Department of Aerospace Engineering, Iowa State University, Ames, IA 50011, USA
Youping Chen, Department of Mechanical and Aerospace Engineering, University of Florida, Gainesville, FL 32611, USA
David L. McDowell, School of Materials Science and Engineering, Georgia Institute of Technology, Atlanta, GA 30332, USA; G.W. Woodruff School of Mechanical Engineering, Georgia Institute of Technology, Atlanta, GA 30332, USA
Liming Xiong, Department of Aerospace Engineering, Iowa State University, Ames, IA 50011, USA

Address all correspondence to Liming Xiong at **lmxiong@iastate.edu**

(Received 30 March 2022; accepted 16 August 2022)

Abstract

We present a phonon dynamics-based finite-temperature coarse-grained (FT-CG) atomistic approach for characterizing the kink-controlled dislocation dynamics in high-Peierls-barrier materials. The applicability of it is demonstrated through simulating the motion of a ~ 3 μm-long dislocation in a bcc iron sample containing ~ 230 million atoms. Cross-kink and debris are found on a μm-long dislocation at a lower stress than that on a nm-long dislocation. They are largely promoted by high-frequency/short-wavelength phonons. FT-CG is shown to be a first model of its kind that can predict the mobility of a μm-long dislocation without smearing out the atomic-level kink dynamics on it.

Introduction

Due to their outstanding mechanical properties, body center cubic (bcc) metals such as iron (Fe) are widely used in engineering infrastructures. However, the fundamental mechanisms controlling their performance when subjected to plastic deformation at finite temperature ($<0.2\ T_m$, where T_m is the melting temperature) is mainly carried by the motion of μm-long ½<111> screw dislocations[1]; (b) the Peierls stress for ½<111> screw dislocations is high and their motion occurs with the aid of the thermally activated atomic-scale kink nucleation and migration[2] for surpassing the high-Peierls barriers of the lattice; (c) the population/activities of kinks vary upon the change of the dislocation line length. As a consequence, the mobility of dislocations in bcc metals is a function of not only the stress and temperature as that in many low-Peierls-barrier materials, but also the line length. Clearly, understanding the dislocation-mediated plastic flow in bcc transition metals demands the formulation and calibration of a dislocation mobility law that incorporates the stress-, temperature-, as well as length dependence all in one analytical form. This is not trivial, especially when we desire to resolve the motion of a μm-long dislocation line while explicitly tracking the kinks along the dislocation line.

Existing approaches used for simulating the motion of screw dislocations in bcc metals mainly fall into two categories. One can be considered as "single-scale" conducted at sub-atomic or atomic-scale resolution, such as density function theory (DFT)[3,4] or molecular dynamics (MD)[5,6] calculations. The other is the fine-scale simulation-informed continuum models, including the DFT-informed line tension (LT)[7] and the atomistic-informed kinetic Monte Carlo (kMC) method.[8] The mobility rules/laws extracted from these approaches are then tested in models at even higher length scales, such as dislocation dynamics (DD)[9–11] or crystal plasticity finite element (CPFE),[12] for simulating the plastic flow in bcc metals at the meso- or macroscopic level. Despite their great success in advancing our understanding about how the kink-controlled dislocation dynamics dictates the plastic flow in bcc metals at finite temperature, the knowledge that has been gained from these approaches should be taken with a certain degree of caution because:

(i) Each single-scale approach was developed at a particular length scale and has its own domain of applicability. For example, although the physics of bonding is reliably reflected in DFT, it is usually only used for a system at zero temperature with a simulation cell being constrained at or below a few nanometers.[3,4] Without accounting for finite-temperature effects, the thermal-induced lattice vibrations which largely reduce the Peierls barrier[13] are missing in DFT. Moreover, by considering tens of or several hundred atoms in the sample with a dimension of only a few nanometers, DFT alone is incapable of describing the kink-pair formation, the occurrence of which spans a length scale of tens of nanometer and even above. Instead, using the interatomic potential, although not as accurate as DFT, MD requires a significantly less computational cost than that of DFT. It can be used for simulating the kink-pair for-

mation on a relatively longer dislocation line at finite temperature.[5,6] The length of the dislocation line that can be considered in MD is, however, still limited to a level of several hundred nanometers. The dynamics of dislocations in such nanoscale MD simulations may be easily affected by the inappropriate boundary/loading conditions[6] and interatomic potentials.[14] The results from MD may not be directly used for interpreting the experimental observations, where only the dynamics of μm-long dislocations can be resolved;[1]

(ii) By contrast, a very long dislocation line can be considered in DFT- or MD-informed LT[7] or kMC[8] models which smear out the atomistic details. For instance, in the DFT-informed LT model,[7] the dislocation is represented by a one-dimensional (1D) elastic line on a substrate carrying a potential, also referred as the Peierls potential (to be extracted from DFT). In this way, it does go beyond the reach of direct DFT calculations when used for characterizing the kink-pair activation enthalpy and kink-pair profile.[7] Similarly, in atomistic-informed kMC models,[8] the dislocations are simplified as a collection of many line segments without considering its atomistic structure. Each segment responds to the stresses according to certain rules, in which a length-/temperature-/stress-dependent kink-pair nucleation probability function is introduced. In this way, the mobility of very long dislocation lines and its dependence on the overall length, stress, and temperature can be then characterized through simulating the collective behavior of many such segments. Such simulations are promising but have a limited predictive capability because they rely strongly on how to implement the information to be averaged from fine-scale simulations. This is challenging especially when the atomic-level kink-pair dynamics and its stress-, length-, and temperature dependence need to be retained.

The development of more realistic dislocation mobility laws for bcc metals necessitates a multiscale model that can accommodate the motion of a μm-long dislocation and the atomic-scale kink dynamics on it within one framework. This model should abandon any assumed rules for describing kink dynamics. It should require the DFT calculation-based data or interatomic potential as the only inputs, while requiring significantly less computation resources than DFT or MD to achieve a seamless length scale-bridging. In this communication, we outline a finite-temperature coarse-grained (FT-CG) approach to simulate the motion of μm-long high-Peierls stress dislocations without sacrificing the physical richness of the atomistically resolved kinks on the dislocation line. This approach is an expansion of our previous model, which we have labeled as Concurrent Atomistic Continuum (CAC)[15–17] through furnishing it with a phonon dynamics-based finite-temperature algorithm. The CAC model was built upon an atomistic field formulation[18] that unifies the atomistic and continuum description of materials starting from the Irving-Kirkwood procedure[19] in statistical mechanics. With the interatomic potential being the only constitutive rule, at a much lower computational cost than that of full MD, our CAC model was shown to have a unique capability of predicting the dynamics of μm-long dislocation lines without smearing out the atomistic core structure on the lines[15–17,20–23]. This paper is structured as follows: the theoretical foundation and numerical implementation of FT-CG are briefly introduced in the Supplemental Material and also "A phonon dynamics-based FT-CG approach" section. To demonstrate its applicability, the FT-CG model set-up and simulation results are presented in "The computer model set-up and simulation results" section. We then conclude this communication with a summary and outlook of this work in "Summary and discussion" section.

A Phonon dynamics-based FT-CG approach

A formulation of Eqs. (1)–(15) (see details in Supplemental Material) and its numerical implementations leads to our FT-CG atomistic model. According to the derivation in the Supplemental Material, a desired temperature of T in our FT-CG simulations is realized through matching the phonon density of states (PDoS) with that from full MD. A first step prior to FT-CG is thus an atomic-level calculation of the material's phonon dispersion relation (also noted as the k-ω relation) or PDoS. Fortunately, for a given material system with a certain crystal structure at a chosen interatomic potential, the k-ω relation and PDoS at certain temperature is always unique and only needs to be calculated once.[24,25] For bcc iron, using the Proville-EAM potential,[14] we first perform a full MD simulation of the dynamic relaxation of a 1,024,000-atom sample for a duration of 200 ps under zero stress at $T=300$ K. An autocorrelation of the atomic velocities from such simulation and its Fourier transformation are then performed. The blue curve in Fig. 1(a) presents the PDoS, noted as, $g(\omega)$, resulting from such a process. Obviously, it has two signatures of the PDoS of a bcc crystal: (a) near the long-wavelength/low-frequency limit, no well-pronounced peaks appears in the vibrational spectra, and $g(\omega)$ is proportional to ω^2; (b) in the short-wavelength/high-frequency domain of $\omega>2$ THz, $g(\omega)$ exhibits three main peaks, which are contributed by the two transverse and one longitudinal phonon modes, respectively. This agrees well with the results from the nuclear resonant inelastic scattering of synchrotron radiation experiments.[26]

These three peaks cannot be readily captured by our previous CAC model.[15–17] The reason is that the coarse-graining procedure in those CAC models cuts off the phonons with wavelengths shorter than λ_c or frequency higher than ω_c. Specifically, $\lambda_c=4h$ if the size of the element chosen for discretization is h. Therefore, it is necessary to include the high-frequency/short-wavelength phonons into CG. These high-frequency phonons can significantly contribute to the kinetic energy of the system and strongly affect the dislocation dynamics in it. In

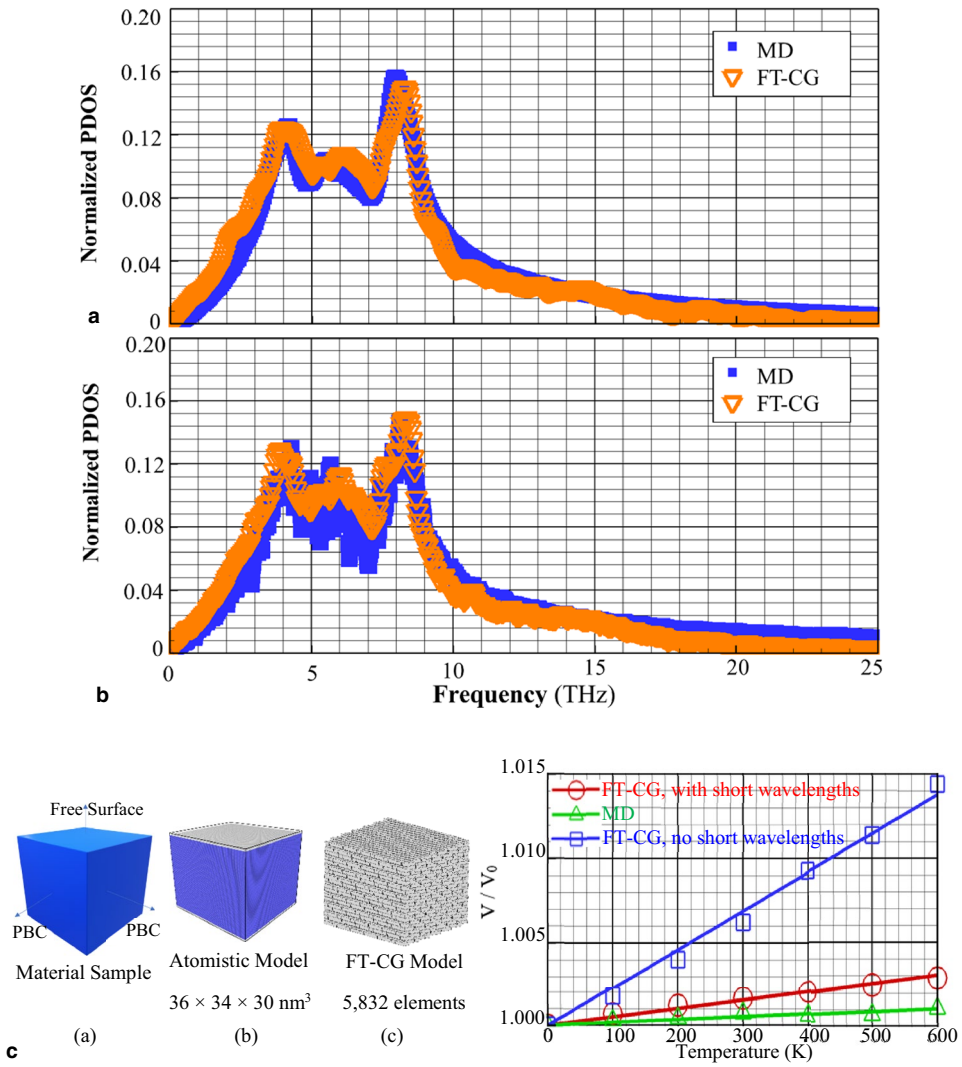

Figure 1. (a) The normalized PDoS, $g(\omega)$, extracted from FT-CG simulations and its comparison with that from full MD simulations of a pristine single crystalline bcc Fe at $T = 300$ K; (b) the PDoS of a single crystalline bcc Fe sample containing a screw dislocation at $T = 300$ K; (c) a prediction of the thermal expansion coefficient of a pristine bcc iron sample through a series of FT-CG as well as full MD simulations showing the change of the sample volume (noted as V) at finite temperature with respect to the sample volume (noted as V_0) at 0 K.

the current FT-CG approach, we correlate the phonon wave dynamics, temperature, the kinetic stress, as well as the internal forces with each other using Eq. (10), Eq. (14), and Eq. (15) in Supplemental Material. This enables the FT-CG to capture the effects of the phonon wave dynamics on the dislocation mobility in an average sense, although not mode specific.

The results obtained from FT-CG simulations are presented in Fig. 1. The orange curve in Fig. 1(a) shows that the PDoS from such a FT-CG (2,000 elements, 512 atoms per element) approach agrees well with the MD simulation-based PDoS. The three peaks which were absent in our previous CG using linear element functions are now captured in this FT-CG. To further validate the predictive capability of such an FT-CG approach, we then introduce a screw dislocation line into the above FT-CG model, but do not change the frequencies and magnitude of the short-wavelength phonons that we have imposed through Eq. (15) (see Supplemental Material). Figure 1(b) reveals that the FT-CG simulation-predicted PDoS of a local domain around the dislocation core is comparable with that from full MD. It uncovers several changes of the PDoS caused by the presence of the dislocation: (i) comparing with the sharp peaks in the PDoS of a pristine crystal [Fig. 1(a)], the peaks in the PDoS for a defected sample [Fig. 1(b)] are seen to be broader due to the occurrence of a dislocation-phonon scattering; and (ii) after the dislocation is introduced, additional peaks (also referred as defect modes) appear in the PDoS as a result of the localized vibration and its interaction with the local stress/strain around the dislocation. Most importantly, comparing with the PDoS of a sample containing no dislocations, the peak

reduction in the PDoS of a bcc iron sample containing a dislocation is negligible. Our recent simulation, however, shows that such a dislocation-induced PDoS peak reduction is notable in bcc tungsten. Accordingly, we believe the dislocation-induced changes in the PDoS in different materials will differ from each other. Overall, the FT-CG provides us with a reliable estimate of the effects of the dislocation on the PDoS. It goes beyond the traditional continuum theories because those theories usually do not have or only have limited resolution near a dislocation core, where the localized lattice vibrations appear and need to be appropriately considered. This will be elaborated in future publications.

In addition to PDoS, the thermal expansion coefficient of bcc iron is also computed from FT-CG and compared with that from full MD simulations. As previously suggested,[27] the thermal expansion coefficient, α, may be used as a metric to assess the entropy loss induced by coarse-graining because phonons with all different wavelengths/frequencies contribute to thermal expansion. For a bcc iron sample exposed to zero stress but different temperatures ranging from 0 K up to 600 K, Fig. 1(c) shows our computer model set-up and the simulation-predicted volume change (noted at V / V_0). The results from the corresponding full MD simulations are also included here for comparison. The sample under consideration here is in a cubic shape with a dimension of 36 nm × 34 nm × 30 nm and contains 3 million atoms. It has free surfaces along z direction. Periodic boundary conditions (PBCs) are imposed along x and y directions [Fig. 1(c)]. In our FT-CG simulations, it is discretized into 5832 coarse FEs (512 atoms per FE). Then the volume change (V/V_0 in Fig. 1) with the increase of the temperatures is measured through a series of FT-CG simulations. Our several major findings from Fig. 1(c) are: (a) the sample volume linearly increases when the temperature increases from 0 to 600 K regardless of whether the FT-CG is enriched with short-wavelength/high-frequency phonons [red curve in Fig. 1(d)] or not [blue curve in Fig. 1(d)]; (b) the slopes of those curves can be estimated as the thermal expansion coefficients, α; **(c)** comparing with the full MD simulations, if only a linear FE shape function is used without any short-wavelength enrichment, α will be largely overestimated using FT-CG; and (d) with the short wavelength being enriched through Eq. (15) in the Supplemental Material, the FT-CG simulation-predicted α [the slope of the red curve in Fig. 1(d)] gets close to that [the slope of the green curve in Fig. 1(d)] from full MD simulations. This implies that the entropy loss, which is unavoidable in the quasicontinuum (QC),[27] has been largely mitigated and can be even eliminated in our FT-CG simulations because all the short-wavelength/high-frequency phonons can be appropriately accommodated.

This is not surprising because several key approximations have been deployed in QC[27] by: (1) choosing a reduced set of representative atoms as an ensemble of nodes suspended in a solvent with all the atomistic DOF in the solvent being neglected; (2) including the effects of the thermal motions of the solvent atoms on the dynamics of the representative atoms into the simulation through introducing a frictional drag; (3) calculating the phonon frequency, ω, the thermal expansion, α, and then the entropy loss within a harmonic framework (See Eqs. (31–49) of[27]); and (4) cutting off the short-wavelength modes, which are present in the underlying atomistics at finite temperature but making no explicit effort to correct the missing entropy induced by an ignore of the short-wavelength vibrations. Distinct from QC, the present FT-CG model is the FE implementation of a full-set governing equations in an atomistic field formulation[18] that unifies the atomistic and continuum descriptions of materials in one framework. It connects the instantaneous atomic forces, displacements, and velocities with the evolution of the field quantities, such as stress and heat flux, at the continuum level. FT-CG considers the thermal effect through Eqs. (13–15) (see Supplemental Material), i.e., a connection between temperature and the kinetic stress. It also does not need any assumed constitutive rules because a link between the divergence of the potential part of the stress and the interatomic forces has been established through Eq. (4) (see Supplemental Material). In this way, FT-CG is fully anharmonic and can produce a thermal expansion coefficient comparable to that from full MD simulations without a notable entropy loss as observed in QC.

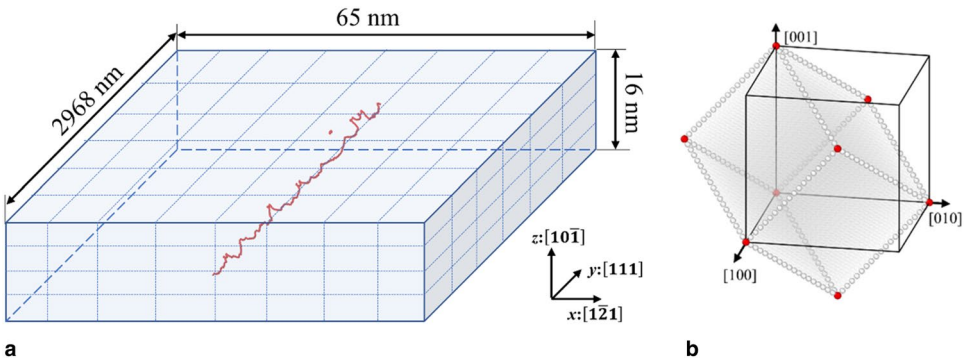

Figure 2. (a) A sketch of the FT-CG model set-up; (b) the FE used for discretizing a bcc crystal.

The computer model set-up and simulation results

FT-CG computer model set-up

The above FT-CG model then provides us with an opportunity to simulate the motion of a dislocation line subjected to both thermal and mechanical stimuli. Figure 2(a) shows the schematic sketch of a FT-CG simulation cell containing a single screw dislocation line. This dislocation line is introduced into the FT-CG models through initially displacing the FE nodes according to the displacement field of a dislocation derived from the theory of elasticity. This dislocation line is oriented along y direction with a slip plane perpendicular to z direction. The PBC is applied along y axis with a dimension of L_y, which is the dislocation line direction. Along x and z direction, the simulation cell is in a dimension of L_x and L_z, respectively, without imposing any PBCs there. With an aim of characterizing the line length dependence of the dislocation motion mechanism, a series of different L_y ranging from 60 to ~3 μm have been considered in this work. In particular, in the FT-CG simulation of the motion of a ~3 μm-long dislocation line, the sample is in a dimension of 65 nm × 2968 nm × 16 nm [Fig. 2(a)]. It contains 230 million atoms but has been discretized into only 450,000 FEs. Here, a specific FE [Fig. 2(b)] with its six surfaces being aligned with the (110) slip planes has been designed for modeling the migration of ½<111> dislocations in bcc metals. Each FE is embedded with 512 atoms. Similar to the strategy used in our previous CAC models,[15–17,20–23,28] the displacement of these 512 atoms within each FE is not explicitly solved and will be interpolated from the FE nodal displacements. Such a set-up brings a two-fold benefit: (i) it requires a significantly less computational resource than that by full MD and thus enables us to study the dynamics of very long dislocation lines; and (ii) it can still retain the atomistic nature of the kink dynamics along the dislocation line when we map the FT-CG simulation-predicted FE mesh configuration into the fully atomic arrangements, from which we can then extract the atomistic details of dislocation line morphology. This is a postprocessing procedure and has been effectively used in our previous CAC simulations[15–17] for elucidating the atomistic details of dislocation activities.

Simulation results

When the sample is subjected to a constant shear, we can track the position of a dislocation line as a function of time, t, in FT-CG simulations. When kink occurs, the dislocation lines in bcc metals can be very rough [Fig. 3(a)]. For measuring the velocity of a rough dislocation line, we can track points along the dislocation front to identify its current position. Figure 3(a) shows a sketch on how the front of a dislocation is selected from the instantaneous configuration of it. Here, the dislocation line is extracted from FT-CG simulations and propagates along x direction. At each time step of the dislocation motion, multiple points along the front of the dislocation line will appear [see the dash blue line in Fig. 3(a)]. Once the positions (noted as $x_1, x_2, \ldots, x_n$) of these points are identified, there are two strategies to calculate the instantaneous velocities. One is $[(x_1+x_2+\ldots+x_n)/n-x_0]/t$, the other is $[\ max\ (x_1, x_2, \ldots, x_n)-x_0]/t$, where x_0 is the initial position of the dislocation line and t is the simulation time when the snapshot is taken. The data based on both of these two strategies are provided in Fig. 3, where solid markers show the data from $[(x_1+x_2+\ldots+x_n)/n-x_0]/t$ and the open markers show the data from $[\ max\ (x_1, x_2, \ldots, x_n)-x_0]/t$. Quantitatively, Fig. 3(b, c) present the results on relating the dislocation velocity, v, with the applied stresses, σ_{ap}, obtained from FT-CG simulations of the motion of a dislocation line with different lengths ($L = 60$ nm and $L = 1000$ nm) when exposed to a temperature of 0.06 T_m and 0.33 T_m. In Fig. 3(b), the horizontal axis is normalized by the Peierls stress, $\sigma_{Peierls}$.

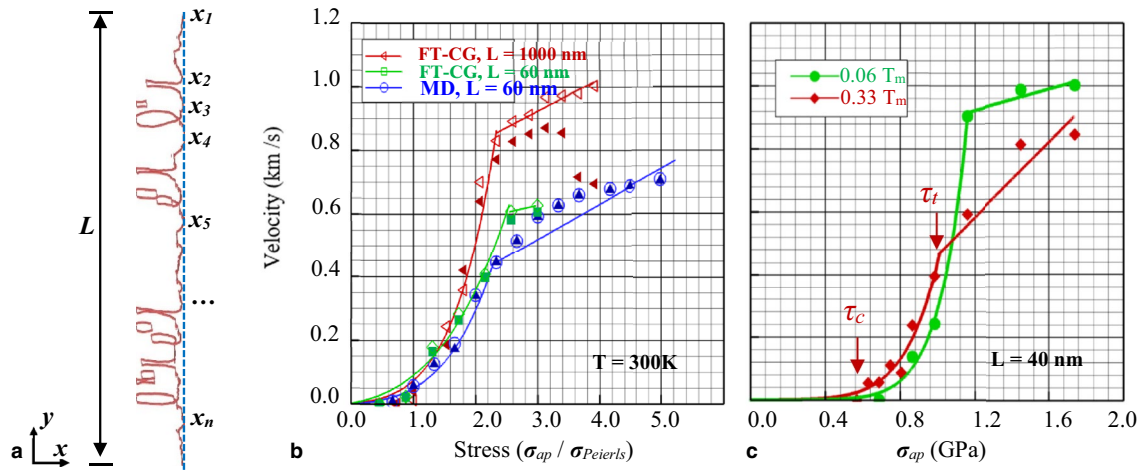

Figure 3. (a) Snapshot of the configuration of a μm-long rough dislocation line extracted from FT-CG simulation and an indication of the "front" of the position ($x_1, x_2, \ldots, x_n$) of the dislocation line along its migration direction; (b) the length-; and (c) temperature dependence of dislocation mobility, i.e., the velocity-stress relation, predicted from the FT-CG and MD.

Several main findings in Fig. 3 are: (1) the FT-CG simulation predicts a velocity-stress relation comparable to that from full MD simulations at $L = 60$ nm [Fig. 3(b)]; (2) it captures the three-regime velocity-stress relation for describing the mobility of screw dislocations in bcc metals. That is, an exponential regime (also known as the thermal activation regime) at low stresses, a linear regime (also known as the viscous or phonon drag regime) at high stresses, and a transition regime in between; (3) the results from the two different velocity measurement strategies don't differ much in both MD and FT-CG simulations [Fig. 3(b)], especially when the dislocation line is not long ($L = 60$ nm); (4) when the dislocation line length is increased up to $L = 1000$ nm, the data from these two different strategies start to diverge from each other [see the open triangles and solid triangles in Fig. 3(b)]. This is reasonable because more cross-kink and self-pinning occur on a longer dislocation line; (5) when exposed to the same temperature [Fig. 3(b)], the longer dislocation always moves faster than the short one in both the thermal activation and phonon drag regimes; (6) when subjected to the same stress, the dislocation line with a length of 40 nm moves faster in the thermal activation regime at a higher temperature than it does at lower temperature. This trend is reversed in the phonon drag regime [Fig. 3(c)]; (7) the critical stress (noted as τ_c) at which the dislocation starts to move reduces upon the increase of the temperature, i.e., $\tau_c \approx 720$ MPa at 0.06 T_m and $\tau_c \approx 560$ MPa at 0.33 T_m [Fig. 3(c)]; and (8) the exponential-to-linear transition stress, noted as τ_t, decreases from ~ 1.2 to 1.0 GPa when temperature is increased from 0.06 to 0.33 T_m [Fig. 3(c)]. These findings are consistent with that from full MD simulations.[6] The capability of the FT-CG simulation in characterizing the stress-, length-, and temperature dependence of a screw dislocation mobility in bcc metals is thus demonstrated.

The FT-CG simulation results in Fig. 3 in turn, provide us with an opportunity of calibrating the phenomenological dislocation mobility laws, such as the one proposed by Gilbert et al.[6] In this mobility law, the v—τ relation in the low-stress regime is expressed as:

$$v = q\sqrt{s}\exp\left[p(1-\sqrt{s})\right] \tag{1}$$

Here, p and q are fitting parameters and $s = \tau/\tau_T(T)$, τ is th external loading and $\tau_T(T)$ is the exponential-to-linear transition stress and $\tau_T(T)$=1370 MPa. In contrast, according to this mobility law, the v—τ relation in the high-stress regime is:

$$v = \frac{\tau b}{B} + v_a \tag{2}$$

where τ is the applied shear stress, b is the Burgers vector of the dislocation, B is the drag coefficient, and v_a is a fitting parameter. When fitting the FT-CG simulation data into Eqs. (1) and (2) for a ~ 3 μm-long dislocation line, the parameters of the mobility laws can be calibrated as: $q = 858.4$ m/s, $p = -5.977$, and $v_a = 682.3$ m/s, respectively. In contrast, when fitting the MD simulation data into Eqs. (1) and (2), for a 60 nm-long dislocation line, the parameters of the mobility laws are: $q = 441.8$ m/s, $p = 5.281$, and $v_a = 184.3$ m/s, respectively. Furthermore, the drag coefficient, B, can be also fit as the inverse of the slope of the velocity-stress relations as shown in Fig. 3. Since the velocity-stress relation is composed of an exponential regime, a linear regime, and a transition regime, the slope of it is obviously not a constant. It exhibits a complex stress-, length-, and temperature dependence. The drag coefficient obtained from our FT-CG simulations by fitting Eq. (2) into the data in the phonon drag regime are 9.54×10^{-3} [Pa s] for $L = 60$ nm and 17.391×10^{-3} [Pa s] for $L = 3$ μm, respectively. Instead, a fitting of Eq. (2) into the data in the transition regime will lead to a drag coefficient as low as 10^{-4} [Pa s], which will be comparable with that from full MD simulations in.[6] Overall, the drag coefficient, B, in Eq. (2) is not simply a constant. It should be formulated as an appropriate function[11] of stress, temperature, and dislocation line length.

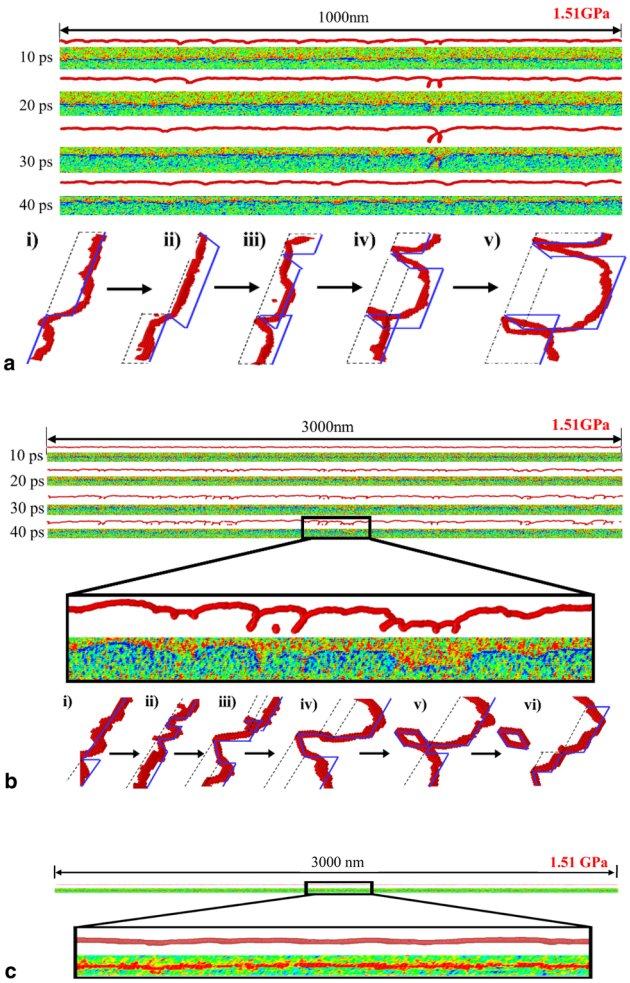

Figure 4. Snapshots of the time sequences of FE configurations during the motion of μm-long dislocation lines together with the atomic-level kink dynamics on the dislocation lines mapped from the FE configurations at τ = 1.51 GPa: (a) $L = 1$ μm by FT-CG with the short-wavelength enrichment; (b) $L = 3$ μm by FT-CG with the short-wavelength enrichment; and (c) $L = 3$ μm by FT-CG without the short-wavelength vibrations being included in the simulation.

Moreover, to demonstrate the capability of the FT-CG simulation in retaining the atomic-sized kink dynamics on a dislocation line, Fig. 4 shows the snapshots of time sequences of FE mesh configurations as well as the dislocation line morphology evolution mapped from the FE mesh configuration during the process of dislocation motion. The results for a 1 μm-long [Fig. 4(a)] and also a ~3 μm-long [Fig. 4(b)] dislocation line are displayed here. During the motion of such μm-long dislocation lines, two dislocation line roughening mechanisms, noted as self-pinning and debris loop formation, are observed. Self-pinning and the subsequent debris loop formation are found to be triggered by the occurrence of cross-kink on a dislocation line as noted before.[1,5,6] In details, they are induced by the screw dislocation line cross-slip to a different plane. The kinks on those two different slip planes may lock with each other and then form a pinning junction for the dislocation motion without the need of any extrinsic obstacles. A detailed analysis of the inset pictures, see (i)-(v) in Fig. 4(a) and (i)–(vi) in Fig. 4(b), confirms that our FT-CG model successfully captures such atomistic details associated with cross-kink, self-pinning, and then debris loop formation. Similar debris loop formation mechanisms in the form of vacancy and interstitial clusters were reported in many previous full MD simulations, although only at the nanoscale. Here, when the dislocation line length is increased up to the ~3 μm level, as shown in Fig. 4(c), the population of kinks and the probability of cross-slip largely increases, which in turn, promotes the cross-kink activities. The interaction among kinks on different planes under such frequent cross-kinks leads to more collisions of kinks. Such collisions lead to the formation of more self-pinning sites. In this scenario, two dislocation line segments may kink further onto the same plane, annihilate with each other, and then leave a small debris loop behind. Interestingly, for Fe at $T = 300$ K, we only observe the debris loop formation during the motion of a ~3 μm-long dislocation lines [Fig. 4(b)] and do not see the debris loop formation during the motion of the 1 μm-long dislocation line [Fig. 4(a)], even though the applied stress is as high as ~1.51 GPa. It suggests that the probability of self-pinning and debris loop formation is significantly higher when the dislocation line is longer.

In other words, the μm-long dislocation lines in bcc metals will be more easily self-pinned than the nm-long dislocation lines. This observation implies: (i) one may not directly inform nanoscale MD simulation-based mobility laws into the mesoscale DD models for describing the collective behavior of μm-long dislocations in bcc metals because the kink-induced self-pinning has been largely suppressed in nanoscale MD simulations; and (ii) the present FT-CG approach can be used as an alternative vehicle of calibrating the mobility laws for describing the kink-controlled dislocation dynamics from the atomistic up to the micrometer level and even above. We also believe that, other than the dislocation line length, another factor which may also contribute to cross-kinking and debris formation is the atomic-level thermal fluctuation near the dislocation core. Such fluctuations give rise to the localized short-wavelength vibration and largely promotes the cross-kinking. To confirm this assertion, Fig. 4(c) presents the results from FT-CG simulations without short-wavelength vibrations being included. For the sample containing a dislocation line under a constant shear of 1.51 GPa, Fig. 4(c) shows that the cross-kinking and debris formation are largely suppressed if the high-frequency/short-wavelength vibration has not been introduced into the FT-CG simulations.

In addition to dislocation line length and high-frequency/short-wavelength phonons, the overdriven dynamics in the computer simulations is of course another important factor contributing to cross-kinking and debris formation. Similar to existing MD simulations, the system in the present FT-CG simulation is still overdriven because: (i) it employs the interatomic potential as the constitutive relation to describe how the materials respond to an imposed stress. For bcc iron, all the existing interatomic potentials, including the one that has been used in this work, estimate a Peierls stress at a level of ~1GPa and above. Thus, the stress imposed on the FT-CG simulation cell has to be at a level of several GPa, which will, of course, strongly drive the dislocation motion as compared to lower experimentally measured values of Peierls stress (tens of MPa) in experiments; (ii) it captures the high-frequency vibrations at THz level through a time integration of the equation of motion. Thus, the time step in the present FT-CG simulations is on the order of fs. Accordingly, the duration of the simulation run can be only up to hundreds of nanoseconds if only modest computational resources are used. Consequently, the strain rates applied in the present FT-CG are still as high as that (10^7–10^9/s) in MD, although the length of a dislocation line in FT-CG can be up to several micrometers. The high strain rate deformation imposed on the sample at a high stress of course will overdrive the system. To suppress or eliminate the effects of such overdriven dynamics, we are working on several strategic directions. First, we can implement a machine-learning (ML) potential which is trained from DFT data. Such a ML potential can simulate an experimentally comparable Peierls stress. We can also pursue a coarse-grained nudged elastic band (NEB) algorithm, which finds the minimum energy pathway between two given states of an interested process (kink-controlled dislocation motion in this work). NEB can be employed using our FT-CG model because the dominant kinematic degrees-of-freedom for kink-controlled dislocation dynamics (cross-kinking, debris formation) are enabled in FT-CG. These dislocation reaction pathways can then be examined using NEB to estimate more realistic transition states and associated activation energies that reflect the influence of both the short- and long-range interactions in FT-CG simulations. A continuous representation of the kinked dislocation configuration is available from FT-CG simulations to serve this purpose. Work on the employment of a ML-based potential in FT-CG is currently underway. In addition, we can consider use of NEB as well to sort out more realistic reaction pathways for an analysis of kink formation and interaction that avoids overdriven conditions. The relevant results will be reported in our future publications.

Summary and discussion

To summarize, here we present a new FT-CG approach for characterizing the kink-controlled dislocation dynamics in bcc transition metals. This approach is built upon the numerical implementation of an Irving-Kirkwood procedure[18,19] which unifies the atomistic and continuum description of materials according to the principles of statistical mechanics. It is an expansion of our previous CAC model[15–17,20–23,28] through the implementation of (i) a new FE set-up to realize a CG description of dislocation migration in bcc crystals, and (ii) a phonon dynamics-based finite-temperature algorithm to resolve the full spectrum of the lattice vibration without cutting off short-wavelength phonons nearby the dislocation core. Taking bcc Fe as an example system, by simulating the motion of a dislocation line with its length ranging from 60 up to ~3 μm, at a fraction of the cost of full MD simulations, with the interatomic potential being the only inputs, the FT-CG approach is shown to be capable of: (a) simultaneously resolving the motion of μm-long dislocation lines as well as the atomic-level kink dynamics (nucleation, migration, annihilation, cross-kink, and so on) on the dislocation lines; (b) characterizing the stress-, temperature-, and the line length dependence of not only the dislocation mobility law, but also the underlying mechanisms from the atomic to the microscale.

This work highlights the feasibility of using FT-CG to: (1) incorporate not only the stress and temperature dependence, but also the dislocation length dependence over a range from tens of nanometers to a few microns, into a generalized dislocation mobility law for bcc transition metals; (2) constructing maps of correlating the dislocation roughening mechanisms, mobility, stress, temperature, as well as the dislocation line lengths all into one diagram. With an ability to simulate a μm-long dislocation while retaining the atomistic nature of kinks along the dislocation line, FT-CG may facilitate a prediction of plasticity in bcc transition metals at an experimentally comparable length scale through informing the FT-CG simulation-based constitutive rules into the higher length scale models, e.g., DD or crystal plasticity finite element (CPFE). In this way, the predictive capability of the continuum model may be significantly improved from the bottom up. The mobility law to be extracted from the FT-CG simulations will be atomistic mechanism-based. It will abandon the parameterization of phenomenological models which are usually fitted from experiments. Such mobility laws will cover a broad length scales. They will introduce the fewest number of degrees-of-freedom while still accurately capture the dynamics of long dislocation lines. For instance, using the FT-CG simulation-based mobility law as an input, DD simulations at millimeter level may become possible by discretizing the long dislocation lines into a large number of μm-long segments, the velocity of which of course needs to be governed by the mobility law calibrated at the micrometer level. In this scenario, if one insists on using the mobility law calibrated from nanoscale MD simulations, the results from DD simulation may be misleading because the length dependence at the micrometer level might significantly differ from that at the nanometer level. Although the atomic-level kink dynamics is not explicitly considered in such DD simulations, an implicit inclusion of kink-pair formation mechanisms into the mobility law through FT-CG simulations can significantly improve the predictive capability of them. Thus, comparing with that from nanoscale MD simulations, the calibration of the mobility of a μm-long dislocation that we have attempted through FT-CG simulations will find applications in DD simulations, and can get one step closer to that in experiments.[1]

Despite its great promise in filling the gap between various single-scale computational models, experiments, and theories, one needs to be cautious about the present FT-CG approach in several aspects. Firstly, the accuracy of FT-CG simulation depends on many factors such as mesh size, mesh shape, and also the interatomic potential used for the FE nodal force calculation. One main factor that might restrict the current FT-CG simulation arises from the FE mesh set-up. Because the dislocations or kinks in the present models are only allowed to occur along the FE boundaries, certain activities might have thus been restricted by the limited number of the slip planes exposed on the present FE boundaries. A wedge- or tetrahedral-shaped or adaptive FE that exposes more slip planes will of course provide us with more flexibilities for capturing even more complex dislocation activities. Also, the constitutive relation, i.e., the underlying interatomic potential, is another factor that can affect the accuracy of FT-CG simulations, especially for the dislocations with non-planar core structures in bcc crystals. For example, the commonly used EAM potentials[14] are not always fully satisfactory in reproducing the dislocation core structures/energetics and their evolution in bcc iron when subjected to stress. Recently, progresses have been made to overcome such issues caused by inaccurate interatomic potentials, such as modified EAM or one of the newest approaches using the machine-learning interatomic potentials[29] to achieve the same accuracy as a density-functional theory, although at a significantly higher computational cost than that by traditional EAM potentials. An implementation of different or adaptive FEs for exposing more slip planes on the element boundaries, together with high-fidelity interatomic potentials, into the present FT-CG models are currently attempted and will be reported in future work.

Acknowledgments

JR, TP, and LX acknowledge the support of the U.S. National Science Foundation (CMMI-1930093 and CMMI-1824840) and the Extreme Science & Engineering Discovery Environment (XSEDE-TG-MSS170003, 190008, and 190013). YC acknowledges the support of the U.S. National Science Foundation (CMMI-1761512). DLM is grateful for the support of the U.S. National Science Foundation (CMMI-1761553) and the Carter N. Paden, Jr. Distinguished Chair in Metals Processing.

Data availability

Data will be made available on reasonable request.

Declarations

Conflict of interest

On behalf of all authors, the corresponding author states that there is no conflict of interest.

Supplementary Information

The online version contains supplementary material available at https://doi.org/10.1557/s43579-022-00238-w.

References

1. D. Caillard, Kinetics of dislocations in pure Fe. Part I: In situ straining experiments at room temperature. Acta Mater. **58**, 3493–3503 (2010)
2. Dorn, J.E. and Rajna, S., 1963. Nucleation of kink pairs and the Peierls mechanism of plastic deformation, Gordon Research Conference, New London, N.H., pp. 10–30.
3. L. Dezerald, L. Proville, L. Ventelon, F. Willaime, D. Rodney, First-principles prediction of kink-pair activation enthalpy on screw dislocations in bcc transition metals: V, Nb, Ta, Mo, W, and Fe. Phys. Rev. B **91**, 094105 (2015)
4. L. Proville, D. Rodney, M.C. Marinica, Quantum effect on thermally activated glide of dislocations. Nat. Mater. **11**, 845–849 (2012)
5. C. Domain, G. Monnet, Simulation of screw dislocation motion in iron by molecular dynamics simulations. Phys. Rev. Lett. **95**, 215506 (2005)
6. M.R. Gilbert, S. Queyreau, J. Marian, Stress and temperature dependence of screw dislocation mobility in α-Fe by molecular dynamics. Phys. Rev. B **84**, 174103 (2011)
7. L. Proville, L. Ventelon, D. Rodney, Prediction of the kink-pair formation enthalpy on screw dislocations in α-iron by a line tension model parametrized on empirical potentials and first-principles calculations. Phys. Rev. B **87**, 144106 (2013)
8. A. Stukowski, D. Cereceda, T.D. Swinburne, J. Marian, Thermally-activated non-Schmid glide of screw dislocations in W using atomistically-informed kinetic Monte Carlo simulations. Int. J. Plast **65**, 108–130 (2015)
9. M. Tang, L.P. Kubin, G.R. Canova, Dislocation mobility and the mechanical response of bcc single crystals: a mesoscopic approach. Acta Mater. **46**(9), 3221–3235 (1998)
10. M. Tang, J. Marian, Temperature and high strain rate dependence of tensile deformation behavior in single-crystal iron from dislocation dynamics simulations. Acta Mater. **70**, 123–129 (2014)
11. G. Po, Y. Cui, D. Rivera, D. Cereceda, T.D. Swinburne, J. Marian, N. Ghoniem, A phenomenological dislocation mobility law for bcc metals. Acta Mater. **119**, 123–135 (2016)
12. S. Narayanan, D.L. McDowell, T. Zhu, Crystal plasticity model for BCC iron atomistically informed by kinetics of correlated kink-pair nucleation on screw dislocation. J. Mech. Phys. Solids **65**, 54–68 (2014)
13. M.R. Gilbert, P. Schuck, B. Sadigh, J. Marian, Free energy generalization of the Peierls potential in iron. Phys. Rev. Lett **111**, 095502 (2013)
14. M.-C. Marinica, L. Ventelon, M.R. Gilbert, L. Proville, S.L. Dudarev, J. Marian, G. Bencteux, F. Willaime, Interatomic potentials for modelling radiation defects and dislocations in tungsten. J. Phys. **25**, 395502 (2013)
15. L. Xiong, G. Tucker, D.L. McDowell, Y. Chen, Coarse-grained atomistic simulation of dislocation. J. Mech. Phys. Solids **59**(2), 160–177 (2011)
16. L. Xiong, D.L. McDowell, Y. Chen, Nucleation and growth of dislocation loops in Cu, Al, and Al by a concurrent atomistic-continuum method. Scripta Mater. **67**(7–8), 633–636 (2012)
17. L. Xiong, R. Ji, X. Chen, S. Xu, D.L. McDowell, Y. Chen, Coarse-grained elastodynamics of fast-moving dislocations. Acta Mater. **104**, 143–155 (2016)
18. Y. Chen, Reformulation of microscopic balance equations for multiscale materials modeling. J. Chem. Phys. **130**(13), 134706 (2009)
19 J.G. Kirkwood, The statistical mechanical theory of transport processes I: general theory. J. Chem.Phys. **14**, 180–201 (1946)
20. L. Xiong, D.L. McDowell, Y. Chen, Sub-THz phonon drag on dislocations by coarse-grained atomistic simulations. Int. J. Plast **55**, 268–278 (2014)
21. S. Xu, L. Xiong, Y. Chen, D.L. McDowell, An analysis of key characteristics of the Frank-Read source process in fcc metals. J. Mech. Phys. Solids **96**, 460–476 (2016)
22. S. Xu, L. Xiong, Y. Chen, D.L. McDowell, Shear stress- and line length-dependent screw dislocation cross-slip in FCC Ni. Acta Mater. **122**, 412–419 (2017)
23. X. Chen, L. Xiong, D.L. McDowell, Y. Chen, Effects of phonons on mobility of dislocation arrays. Scripta Mater. **137**, 22–26 (2017)
24. M.T. Dove, *Introduction to Lattice Dynamics* (Cambridge University Press, Cambridge, 1993)
25. L.T. Kong, Phonon dispersion measured directly from molecular dynamics simulations. Comput. Phys. Commun. **182**, 2201–2207 (2011)
26. R. Meyer, L. Scherthan, T. Hochdorffer, S. Sadashivaiah, J.A. Wolny, M.W. Klein, M. Smaga, T. Beck, V. Schunemann, H.M. Urbassek, Changes in the phonon density of states of Fe induced by external strain. Appl. Phys. A **127**, 5 (2021)
27. J. Marian, G. Venturini, B.L. Hansen, J. Knap, M. Ortiz, G.H. Campbell, Finite-temperature extension of the quasicontinuum method using Langevin dynamics: entropy losses and analysis of errors. Modell. Simul. Mater. Sci. Eng. **18**, 015003 (2010)
28. X. Chen, A. Diaz, L. Xiong, D.L. McDowell, Y. Chen, Passing waves from atomistic to continuum. J. Comput. Phys. **354**, 393–402 (2018)
29. F. Maresca, D. Dragoni, G. Csanyi, N. Marzari, W.A. Curtin, Screw dislocation structure and mobility in body centered cubic Fe predicted by a Gaussian approximation potential. NPJ Comput. Mater. **4**, 69 (2018)